RESEARCH PAPER

Enhancing peripheral nerve regeneration: A novel nanofibrous nerve conduit with bioactive poly(ε-caprolactone), collagen, and retinoic acid nanofiber

Muhammad Aseer [1]*, Niloofar Nazeri [2], Nasrollah Tabatabaei [1], Zohreh Arabpour [3], Reza Faridi Majedi [1], Hossein Ghanbari [1, 4]*

[1]Department of Medical Nanotechnology, School of Advanced Technologies in Medicine, Tehran University of Medical Sciences, Tehran, Iran
[2]Cellular and Molecular Research Center, Qazvin University of Medical Sciences, Qazvin, Iran
[3] Department of Ophthalmology and Visual Sciences, University of Illinois at Chicago, Chicago, IL, USA
[4] Institute of Biomaterials, University of Tehran & Tehran University of Medical Sciences (IBUTUMS), Tehran, Iran

ABSTRACT

Objective(s): Peripheral nerve injury (PNI) is a critical clinical issue primarily caused by trauma. Tissue engineering approaches using nanofiber scaffolds have been extensively explored to improve material quality and create an environment resembling the natural extracellular matrix (ECM).

Materials and Methods: In this study, we employed electrospinning technique to fabricate a composite scaffold comprising poly(ε-caprolactone) (PCL) and collagen (Col) loaded with all-trans retinoic acid (RA), a neural patterning and signaling chemical known to promote nerve regeneration.

Results: The synthesized nanofiber scaffold exhibited a diameter of 391±79 nm and a tensile strength of 250±13 MPa, providing sufficient support for native peripheral nerve regeneration. The inclusion of Col enhanced the scaffold's hydrophilic behavior (contact angle: 43±6°), ensuring stability in an aqueous solution. Moreover, the results demonstrated the proliferation and adhesion of nerve cells on the scaffold, aligning with the directions of the warp and weft of the nanofiber mat. Importantly, the scaffolds demonstrated non-toxicity, making them a promising substitute for the native ECM for enhanced cell attachment and proliferation. Finally, immune-histochemistry analyses further confirmed that the scaffolds supported the release and growth of neurites, promoting cell differentiation toward nerve repair.

Conclusion: The RA-loaded scaffolds demonstrated the enhanced biocompatibility, supported neurite growth, and showed potential as a capable candidate for nerve regeneration.

Keywords: *Collagen, Electrospinning, Nerve cells, Nerve regeneration, Poly(ε-caprolactone), Retinoic acid*

How to cite this article
Aseer M, Nazeri N, Tabatabaei N, Arabpour Z, Faridi Majedi R, Ghanbari H. Enhancing peripheral nerve regeneration: A novel nanofibrous nerve conduit with bioactive poly(ε-caprolactone), collagen, and retinoic acid nanofiber. Nanomed J. 2025; 12(1):42-50. DOI: 10.22038/nmj.2024.77144.1878

INTRODUCTION

Peripheral nerve injury (PNI) is a pressing medical and public health concern, often leading to significant loss of function and permanent disability [1]. Traumatic incidents are the primary cause of PNI, but it can also result from degenerative syndromes or damage due to thermal, chemical, mechanical, or ischemic factors [2-4]. The severity of PNI is typically evaluated using classifications such as Seddon's neurapraxia, axonotmesis, and neurotmesis, or Sunderland's grading system [5-7]. However, regardless of the classification, the breakdown of axons and myelin at the injury site triggers Wallerian (anterograde) degeneration, disrupting the connection between the distal end and the main neural body [9].

Current medical therapies for PNI, such as end-to-end repair, are effective for small nerve gaps but not practical for significant gaps. In such cases, nerve autografts have been considered the "gold standard" treatment, but they come with donor site morbidity concerns. Consequently, researchers have turned to tissue engineering approaches to develop artificial nerve guidance

* *Corresponding authors: Emails: hghanbari@tums.ac.ir; m-aseer@razi.tums.ac.ir*
Note. This manuscript was submitted on December 27, 2023; approved on April 2, 2024

conduits (NGCs) that can bridge nerve gaps and support axonal regrowth [10-12].

Among these approaches, nanofiber-based NGCs have shown promise as a potential replacement for autografts. They offer the advantage of immediate availability when on-the-spot autografts are not feasible and act as barriers to scar tissue formation [13]. Successful nerve regeneration through artificial conduits relies on factors such as the gap to be bridged and the physical and material characteristics of the NGCs. Ideal conduits should possess biocompatibility, high porosity, neuro-inductivity, suitable physio-chemical properties, and an appropriate degradation rate [16]. Moreover, parameters like the internal diameter of the conduit and permeability of the outer wall can also influence the outcomes of the NGCs [9, 10].

To enhance the cell adhesion properties of NGCs, investigators have designed composite conduits using a combination of natural and synthetic polymers. Biodegradable synthetic polymers have gained traction due to their biocompatibility, non-immunological responses, mechanical properties, controlled degradation rates, and a wide range of material choices [21-23]. Additionally, the incorporation of bioactive molecules in tissue engineering, such as retinoic acid (RA), has shown promise in enhancing scaffold bioactivity and supporting cellular activities to promote tissue regeneration [24-29].

In this study, our focus was on developing a novel bioactive nanofibrous scaffold based on poly(ε-caprolactone) (PCL) and collagen (Col) encapsulating RA. RA has demonstrated the ability to regulate cellular behavior and enhance the differentiation of neural cells, promoting cells growth and controlled proliferation. Moreover, RA stimulates neuronal expression, supporting neural patterning and signaling to promote myelination and axonal growth during nerve repair.

Our primary objective was to fabricate an RA-loaded nanofibrous scaffold (PCL/Col/RA) and evaluate its potential as a bio-construct for peripheral nerve regeneration. Specifically, we investigated the biocompatibility of nerve cells (PC12) with the proposed scaffold and assessed its ability to support cell migration, adhesion, proliferation, and nerve cell neurite formation and extension. By addressing these considerations, we aim to contribute to the advancement of nanofiber-based nerve conduits, potentially providing a promising alternative to autografts for promoting nerve regeneration and functional recovery in patients with PNI.

MATERIALS AND METHODS

Extraction of collagen

Collagen type-I (Col) was extracted from the rat tails. The Tehran University of Medical Sciences Animal Center's Pharmacy Department supplied the rats' tails. All these rate tails were kept at -20 °C prior to being used to extract collagen. After removing the rat tails from the -20 °C extraction, they were put in a 1000 mL beaker under the biosafety hood after spraying them with 70% alcohol. After ten minutes, the rat tails were cut into small pieces. Collagen extract needs to be gathered in a different beaker containing distilled water. Eight to ten rat tails and 800-1000 mL of distilled water were added to a beaker containing isolated collagen. Following the extraction process, the collagen was rinsed two or three times with distilled water. Next, 0.01% of acetic acid was added to the 1000 mL of collagen solution, followed by mixing and keeping at 4 °C for 24 hr. The following day, the collagen solution was centrifuged for 40 minutes at 8000–1000 rpm. After that, the pure collagen solution was poured into 50 mL flasks and was frozen at -75°C. To obtain the final collagen product, the collagen solution was dried, frozen, and then, stored at 20 °C for the intended uses.

Nanofiber fabrication

Type-I Col was extracted from rat tails, and all-trans-RA, PCL (Mn: 70,000), absolute acetic acid, and methanol were procured from Sigma Aldrich (USA). For the fabrication of PCL/Col nanofiber scaffolds, separate solutions (11% w/w, 50:50) for PCL and collagen were prepared. PCL was dissolved in absolute acetic acid, while Col was dissolved in acetic acid 90% aqueous solution; both subjected to stirring for 2 hr at room temperature. To obtain the final PCL/Col blend, the two solutions were mixed and stirred for an additional 30-45 min at room temperature. Subsequently, the PCL/Col blend was loaded into a syringe for electrospinning. The electrospinning process was carried out under optimized parameters, including 16-18 kV voltage, a 10 cm distance between the syringe tip and the collector, and a syringe pump flow rate of 1 mL/h.

For the preparation of PCL/Col/RA blend, a previously reported 11% w/w (50:50) PCL solution

was utilized. A stock solution of RA (3 mg/mL in MeOH) was prepared, and a 0.3% formulation of RA from this stock was added to the PCL solution at room temperature. The mixture was stirred for 24 hr. Additionally, a separate 11% w/w solution of Col was dissolved in acetic acid 90% aqueous solution and stirred for 2 hr. The PCL/Col/RA blend was obtained by mixing both solutions and stirring for 30-45 minutes at room temperature. The blend was electrospun using the same parameters as the PCL/Col nanofiber scaffolds. Each nanofiber scaffold was designed with 5-6 mL of solution, and both PCL/Col and PCL/Col/RA nanofiber scaffolds were dried for further characterization [30-36].

Cross-linking of scaffolds

To stabilize the nanofibers on the scaffolds, cross-linking was performed. The nanofiber scaffolds were exposed to 25% glutaraldehyde (GA) vapor in a desiccator at room temperature for 3 hr [37, 38].

Characterization of nanofiber scaffolds

2.4.1 Morphology Analysis

Scanning electron microscopy (SEM, XL 30; Philips, Amsterdam, Netherlands) was employed for morphological investigations of the nanofiber scaffolds after sputter coating with gold at 25 kV. The size (diameter) and porosity of the nanofibers were measured using ImageJ software (Image J; US NIH, Bethesda, MD, USA) by randomly selecting 25 points in each sample [38, 39].

Measurement of contact angle

The wettability of the nanofiber scaffolds was assessed using an optical water contact angle measurement device (OCA-15-plus, Data Physics). A 2 × 3 cm^2 sample was placed on the measuring instrument's surface. A deionized water drop (6-10 µL) was placed on the sample using a pipette tip, and the contact angle was analyzed using a high-resolution camera. Average values were obtained from at least three measurements for each scaffold [40].

Mechanical analysis

The mechanical properties of the nanofiber scaffolds were determined using a mechanical testing device at room temperature. The samples were placed between two mechanical clamp units, and tensile analyses were performed at an extension rate of 5 mm/min. The ultimate tensile strength, elongation at break, and modulus of elasticity were calculated from stress-strain curves for each sample (n=3) [38, 41].

Chemical characteristics

The presence of specific chemical functional groups in the nanofiber composites was determined using Fourier-transform infrared (FT-IR) spectroscopy. FT-IR spectra were obtained for pure PCL/Col nanofibers and RA-loaded PCL/Col nanofibers in the range of 4000-600 cm^{-1} [38, 42-44].

Evaluation of scaffold biodegradability

To assess changes in nanofiber content in an aqueous solution, samples with an initial weight (W0) were stirred and incubated in phosphate-buffered saline (PBS) at pH 7.4 and 37 °C, with agitation at 100 rpm for 4 weeks. Throughout the experiment, the PBS solution was not renewed, but samples were aspirated at specific time points, cleaned with distilled water, dried, and weighed to obtain the final weight (Wt). The remaining mass percentage for each sample was calculated using the following equation [39, 40].

$$\text{Remaining mass \%} = (Wt / W0) \times 100$$

In-vitro cell study

Nanofiber scaffolds were initially made according to the dimensions of a 48-well plate before beginning the cell culture. Subsequently, the samples were washed with 70% alcohol and exposed to UV light for half an hour on each scaffold side. Samples were UV sterilized, and then, cleaned three times using sterile PBS and finally used for cell culture procedures. PC12 cells were cultured in RPMI supplemented with 10% fetal bovine serum (FBS) and 1% penicillin/streptomycin at 37 °C, 95% humidity, and 5% CO_2 in a 25 cm^2 flask. After reaching a density of 4×105 cells/well, the cells were seeded in complete medium in 48-well plates for analysis. The biocompatibility of cells with fiber scaffolds was assessed using the Alamar Blue® assay at days 1, 3, 5, and 7. Absorbance at 570 nm was measured in triplicate (n=3) for each sample and time point, and the results were standardized for PC12 cell growth on scaffolds [43].

Cell adhesion study

SEM measurements were performed to assess

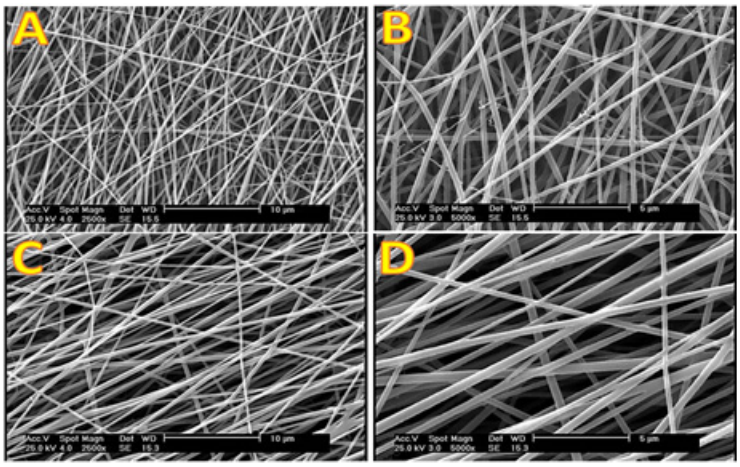

Fig. 1. (A, B). SEM images of aligned PCL/Collagen nanofibers, scale bar = 10µm & 5 µm, (C, D). SEM images of aligned PCL/Collagen/RA nanofibers, scale bar = 10µm & 5 µm

the morphological changes of PC12 cells on the scaffolds at 1 and 7 days of treatment. The cell-seeded scaffolds were rinsed with PBS, fixed with 4% paraformaldehyde for 30-45 minutes, and then, dehydrated with increasing ethanol concentrations (50%-100%) for 15 minutes. The scaffolds containing cells were air-dried for 24 hr at room temperature, gold-sputtered, and examined with a scanning electron microscope (Philips XL-30, Netherlands) at 25 kV [45].

Immunostaining

PC12 cells were fixed with 4% paraformaldehyde for 10 minutes, rinsed with PBS, and stained with anti-beta-tubulin monoclonal antibodies (1:100) and secondary antibodies conjugated to fluorescein isothiocyanate (FITC) at 2-80 °C for 1 hr. After washing, the cells were treated with a diluted goat serum secondary antibody (1:150) and incubated for 90 minutes at 37 °C. Following additional washings and DAPI staining, the samples were examined under fluorescence microscopy. The number of differentiated cells was determined by counting cells with at least one neurite longer than the cell body diameter, and the number of elongated neurites per cell was calculated [46].

Statistical analysis

GraphPad Prism9 software was used for statistical analysis using one-way analysis of variance (ANOVA). Data were presented as mean ± standard deviation (n=3). Statistical significance was set at $p < 0.05$ for all analyses.

RESULTS

Morphology Study of Nanofibers

The electrospinning technique was employed to fabricate PCL/Col and PCL/Col/RA scaffolds composed of nanofibers with size distribution in the nanometer range. SEM images of PCL/Col nanofibrous scaffolds (Fig. 1A, B) and PCL/Col/RA nanofiber scaffolds (Fig. 1C, D) collected on a high-speed rotating cylindrical mandrel demonstrated the average diameter of nanofibers to be 367±45 nm and 391±79 nm for PCL/Col and PCL/Col/RA, respectively.

Moreover, the porosity of PCL/Col (51.85±4%) and PCL/Col/RA (58.45±3%) nanofiber scaffolds was measured, indicating their potential to mimic the natural ECM for cellular interactions.

Contact angle measurement

Contact angle measurements were obtained for PCL/Col and PCL/Col/RA nanofiber scaffolds to assess their hydrophilicity. The observed contact angles were 37±9° and 43±6° for PCL/Col and PCL/Col/RA, respectively, confirming the hydrophilic behavior of the materials.

Tensile testing

Mechanical resistance is a crucial parameter in the construction and design of nanofiber scaffolds. Young's modulus, ultimate tensile strength (UTS), and strain at break were evaluated to assess the mechanical properties of the nanofiber scaffolds (Table 1). The mechanical characteristics of the PCL/Col and PCL/Col/RA groups have different results but still they did not significantly differ from one another. According to the observed data, Young's modulus of PCL/Col scaffold (9.03±0.22 MPa) was comparable to PCL/Col/RA (8.69±0.18 MPa). In addition, the UTS of Electrospun PCL/Col (4.6±0.63 MPa) was also comparable to that of

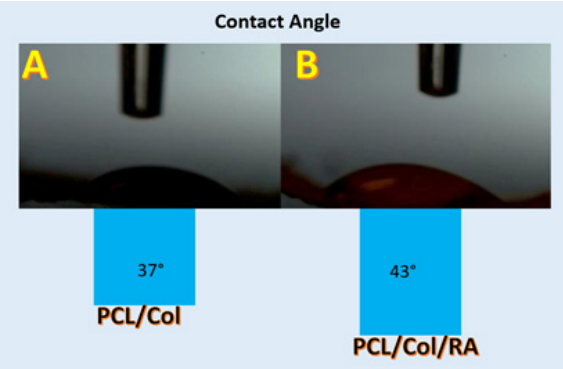

Fig. 2. Contact Angle Measurements of PCL/Coll & PCL/Coll/RA scaffolds

PCL/Col/RA (3.3±0.71 MPa).

FT-IR analysis

The comparison of FT-IR spectra between pure PCL/Col and PCL/Col/RA nanofibers provided valuable insights into potential modifications resulting from the encapsulation of drugs within PCL/Col nanofiber carriers. The FT-IR spectrum of the PCL/Col blend (Fig. 3a) showed the characteristic bands, such as N-H stretching at 3302 cm^{-1} for amide A, C-H stretching at 3068 cm^{-1} for amide B, C=O stretching at 1600–1700 cm^{-1} for amide I, N-H deformation at 1500–1550 cm^{-1} for amide II, and N-H deformation at 1200–1300 cm^{-1} for amide III. The presence of additional distinctive peaks of collagen at 1538 cm^{-1} for amide II (N-H deformation), 3068 cm^{-1} for amide B (C-H stretching), and 3302 cm^{-1} for amide A (N-H stretching) confirmed the composition of the polymeric blend made of PCL and collagen [47-50]. In the PCL/Col/RA blend (Fig. 3b), no new peak was observed, indicating that the amount of RA in the blend did not significantly alter the PCL/Col functional groups [47].

Degradation analysis

Fig. 4 presents the results of scaffold degradation. Degradation commenced from the first week of treatment for both scaffolds, with faster degradation observed during the initial week. Notably, PCL/Col/RA showed a higher degradation rate than the PCL/Col scaffold, possibly due to RA fibers being more susceptible to hydrolytic breakdown than PCL/Col fibers.

In-vitro cytotoxicity test

Fig. 5 depicts the biocompatibility and cytotoxicity of PCL/Col and PCL/Col/RA scaffolds at 1, 3, 5, and 7 days using Alamar Blue® assay. PC12 cells cultivated on the nanofiber scaffolds demonstrated the cell proliferation and viability

Table 1. Tensile properties of PCL/Col, and PCL/Col/RA nanofibrous scaffolds

Sample	Young's Modulus (MPa)	Ultimate Tensile Strength (MPa)	Strain at Break (%)
PCL/Col	9.03±0.22	4.6±0.63	300±16.2
PCL/Col/RA	8.69± 0. 18	3.3±0.71	250±13.4

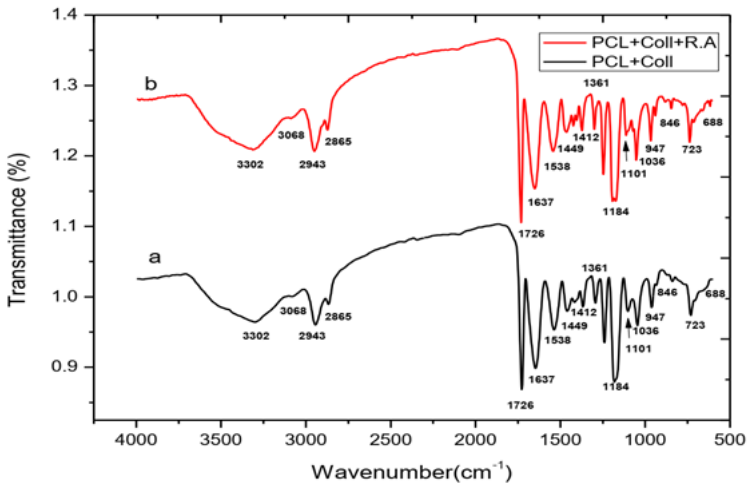

Fig. 3. FTIR spectra of (A) PCL/Col and (B) PCL/Col/RA nanofibers

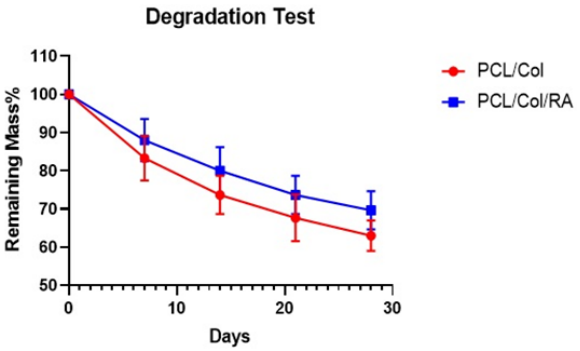

Fig. 4. Degradation analysis of PCL/Col & PCL/Col/RA scaffolds

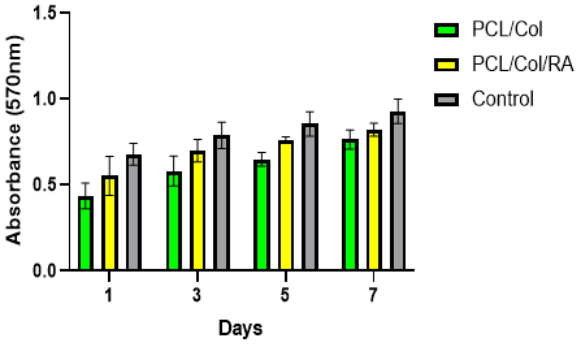

Fig. 5. Alamar Blue assay of PC12 cells on PCL/Col & PCL/Col/RA scaffolds

similar to the control group with no significant changes. Both the RA-loaded and PCL/Col scaffolds were non-toxic to nerve cells.

Cell adhesion study

Cell adhesion to the scaffold is crucial for nerve regeneration. SEM analyses of cell adherence to PCL/Col and PCL/Col/RA scaffolds on day 1 and day 7 are shown in Fig. 6 (A, B) and (A, D), respectively.

Immunochemistry analysis

Immunofluorescence staining of α-Tubulin was used to evaluate its impact on cell differentiation. Cells grown on multiple scaffolds expressed the α-Tubulin protein, with PCL/Col/RA scaffolds promoting more neurite outgrowth compared to PCL/Col scaffolds (Fig. 7).

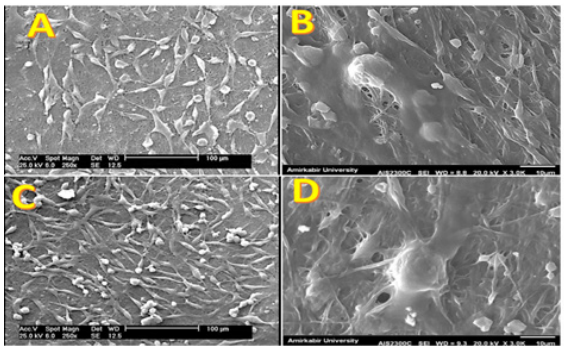

Fig. 6. SEM images of cell adhesion (A) PCL/Col in days 1, (B) PCL/Col/RA in days 1, (C) PCL/Col in days 7, (D) PCL/Col/RA in days 7

DISCUSSION

In regeneration applications, the use of nanofiber scaffolds as nerve conduits is becoming more and more important. Because they offer a favorable microenvironment for the regeneration of nerves. The results of this study indicate that the likelihood of successfully fabricating nanofibrous biomaterial scaffolds from synthetic and biopolymers may be increased by using an

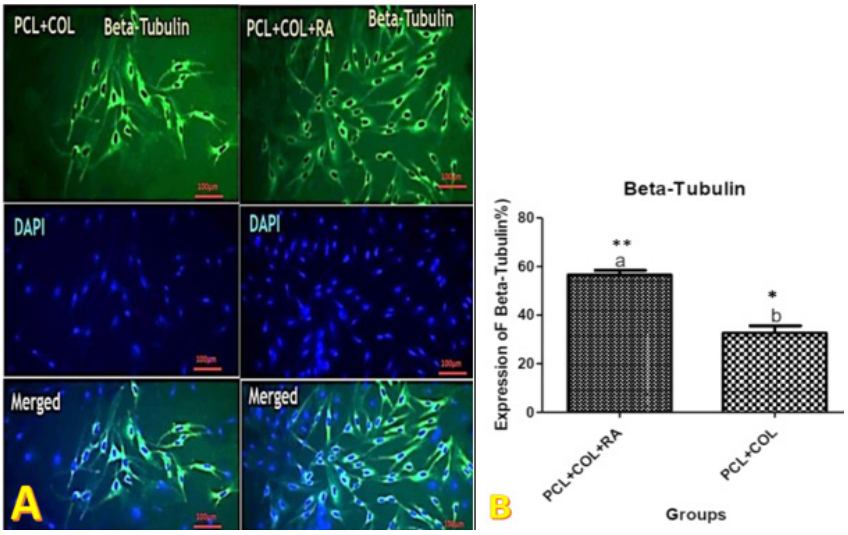

Fig. 7. (A, B): Immunochemistry of PC12 on PCL/Col and PCL/Col/RA scaffolds with anti-tubulin peptide antibodies to evaluate α-tubulin protein expression

electrospinning technique. The diameter, size distribution, and orientation are determined by the polymer concentration and the speed at which the electrospinning collector rotates [51]. For instance, it is possible to create more uniform fibers by raising the spinning speed. The optimal rotation speed for the 11% (50:50) (w/w), PCL/Col and PCL/Col/RA solutions was 2500 rpm. The previous research has shown that nerve cell attachment and neurite extension along nanofiber alignment are important factors in nerve cell neurite growth [52].

Nanofiber morphology, size, alignment, and porosity play an important role in cell adhesion, migration, and proliferation. SEM images showed that PCL/Col and PCL/Col/RA solutions with 11% (50:50) (w/w) might produce nanofibers with exceptional morphology. Additionally, while creating a tissue-engineered scaffold, porosity is an important consideration. In addition to facilitating enough gas and nutrition exchange for wound healing, porous design is critical for encouraging cell infiltration and proliferation. Between 50 and 90 percent porosity is the ideal range for scaffolds used in cellular penetration [53]. The results revealed the nanofibers with an excellent porosity and alignment that provides enough neurites for axonal regeneration.

As mentioned before, surface chemistry, shape, and material composition of the scaffold all affect hydrophilicity. Although PCL is hydrophobic by nature, it becomes hydrophilic when mixed with collagen, as shown in Fig. 2. Our results demonstrates that in PCL/Col/RA scaffolds containing all-trans-retinoic acid, the water contact angle increases in comparison to PCL/Col alone. The results show that both scaffolds are hydrophilic in the presence of Col and RA. Mechanical study found that both groups could withstand tensile stress. In actuality, the tests showed that the elongation at break of the PCL/Col/RA polymer matrix was comparable to that of PCL/Col. According to this, PCL/Col based composite nanofibers are more resilient to force stretching and more appropriate for use as nerve conduits in-vivo [53].

As the frequency of vibration of the groups involved in hydrogen bond production lowers, FT-IR's sensitivity to hydrogen bonds causes a redshift in the functional group. The research has shown that drug solubility in the polymer matrix may be enhanced by hydrogen bonding between the drug and the polymer matrix [53] and prohibits drug re-crystallization in nanofibers [53]. The presence of infrared absorption of PCL groups in the spectra of PCL/Col/RA (containing the drug) suggests that the structural molecules in the fibers were conserved during the electrospinning process, as did the absence of a new band for the drug RA, important for producing the current polymeric drug delivery systems.

Degradation studies indicate that PCL/Col/RA is a better option than PCL/Col for regeneration applications. This is because RA degrades more slowly in an aqueous solution and has a higher stability [54]. Stated differently, compared to PCL/Col nanofibers, the RA-based PCL/Col construct exhibits greater stability and persistent degradability [3]. Furthermore, there was reduced edema in the RA-based combo, which could speed up the regeneration process.

In-vitro data reveal that planted cells disseminate effectively and adhere well to PCL/Col and PCL/Col/RA scaffolds. Fig. 6 shows the adherence and spreading of cells along the alignment of PCL/Col/RA nanofibers.The findings support prior research suggesting that incorporating RA into nanofibrous scaffolds could promote cell growth [55]. Hence, cell study results confirmed the biocomatibity of the fabricated construct towards neural regneration. After confirming the cellular viability on the scaffolds, neurite outgrowth was studied to determine how varied surface chemistries and fiber orientations influence neurite cellular elongation and orientation, as well as extension ratio [43-46].The immunochemistry study revealed that neurites released from PCL/Col/RA scaffolds and neurite development was sufficient and active enough to promote cell differentiation for peripheral nerve damage. Furthermore, it has been demonatrated that the number of neurites growing in PCL/Col/RA is twice that of neurites growing in PCL/Col scaffolds, as shown in Fig. 7.

CONCLUSION

Materials with nanofibrous scaffolds show promise for effective axonal development and nerve healing. For nerve cell formation and axonal regeneration, the electrospinning of RA-loaded PCL/Col offered a high surface area, sufficient mechanical strength, hydrophilic behavior, and a tailored degradation rate. A biomimetic milieu was also produced by loading RA as an efficient

therapeutic drug for nerve cell adhesion and proliferation on scaffolds. By allowing for enough neurite extension for axonal growth, this design may prevent the production of ingrowth fibrous scar tissue. According to the initial findings, PCL/Col/RA-based nanofibrous conduits may offer feasible biological cues and topography for tissue engineering and peripheral nerve regeneration.

Indisputably, new therapeutic approaches that promote nerve regeneration will contribute to the development of artificial implants that act as nerve guides for peripheral nerve repair. To advance this research, however, more investigation into related techniques may be necessary that underpin the creation of a bioimplant. These techniques include the design and construction of scaffolds that mimic in-vivo and *ex-vivo* nerve tissue, as well as the induction of tissue-engineered scaffolds through the implantation of 3D-cultured nerve cells.

FUNDING AND ACKNOWLEDGEMENTS

This research project was sponsored by "Tehran University of Medical Sciences (TUMS)" with grant number IR.TUMS.MEDICINE.REC.1399.478**.** The authors declare no conflict of interest.

CONFLICT OF INTEREST

The authors declare that they have no known competing financial interests or personal relationships that could have appeared to influence the work reported in this paper.

REFERENCES

1. Robinson LR.Traumatic injury to peripheral nerves. Muscle Nerve. (2022); 66(6): 661-670.
2. Taylor CA, Braza D, Rice JB, Dillingham T. The incidence of peripheral nerve injury in extremity trauma. Am J Phys Med Rehabil. 2008; 87(5):381-385.
3. Evans GR. Peripheral nerve injury: a review and approach to tissue engineered constructs. Anat Rec. 2001;263(4):396-404.
4. Robinson LR. Traumatic injury to peripheral nerves. Suppl Clin Neurophysiol. 2004;57:173-186.
5. Bridge PM, Ball DJ, Mackinnon SE, Nakao Y, Brandt K, Hunter DA, Hertl C. Nerve crush injuries—a model for axonotmesis. Exp Neurol. 1994;127(2):284-290.
6. Sunderland S. A classification of peripheral nerve injuries producing loss of function.Brain. 1951;74(4):491-516.
7. Campbell WW. Evaluation and management of peripheral nerve injury. Clin Neurophysiol. 2008;119(9):1951-1965.
8. Seddon HJ, Medawar PB, Smith H. Rate of regeneration of peripheral nerves in man. J Physiol. 1943;102(2):191.
9. Deumens R, Bozkurt A, Meek MF, Marcus MA, Joosten EA, Weis J, et al. Repairing injured peripheral nerves: bridging the gap. Prog Neurobiol. 2010;92(3):245-276.
10. Arslantunali D, Dursun T, Yucel D, Hasirci N, Hasirci VJ. Peripheral nerve conduits: technology update. Med Devices (Auckl). 2014:405-424.
11. Muheremu A, Ao Q. Past, present, and future of nerve conduits in the treatment of peripheral nerve injury. International BR. 2015;2015(1):237507.
12. Houshyar S, Bhattacharyya A, Shanks R. Peripheral nerve conduit: materials and structures. ACS Chem Neurosci. 2019;10(8):3349-3365.
13. Potucek RK, Kemp SW, Syed NI, Midha R. Peripheral nerve injury, repair, and regeneration. InStrategies in Regenerative Medicine: Integrating Biology with Materials Design. Springer. 2008:1-20.
14. Lundborg G. A 25-year perspective of peripheral nerve surgery: evolving neuroscientific concepts and clinical significance. J Hand Surg Br. 2000;25(3):391-414.
15. Pabari A, Lloyd-Hughes H, Seifalian AM, Mosahebi A. Nerve conduits for peripheral nerve surgery. Plast Reconstr Surg. 2014;133(6):1420-1430.
16. Yan Y, Yao R, Zhao J, Chen K, Duan L, Wang T, et al.Implantable nerve guidance conduits: Material combinations, multi-functional strategies and advanced engineering innovations. Bioact Mater. 2022;11:57-76.
17. Zarrintaj P, Zangene E, Manouchehri S, Amirabad LM, Baheiraei N, Hadjighasem MR, et al. Conductive biomaterials as nerve conduits: recent advances and future challenges. Appl Mater Today. 2020;20:100784.
18. Singh D, Harding AJ, Albadawi E, Boissonade FM, Haycock JW, Claeyssens F. Additive manufactured biodegradable poly (glycerol sebacate methacrylate) nerve guidance conduits. Acta Biomater. 2018;78:48-63.
19. Itai S, Suzuki K, Kurashina Y, Kimura H, Amemiya T, Sato K, et al. Cell-encapsulated chitosan-collagen hydrogel hybrid nerve guidance conduit for peripheral nerve regeneration. Biomed Microdevices. 2020;22:1-9.
20. Abidian MR, Daneshvar ED, Egeland BM, Kipke DR, Cederna PS, Urbanchek MG. Hybrid conducting polymer–hydrogel conduits for axonal growth and neural tissue engineering. Adv Healthc Mater. 2012; 1(6):762-767.
21. Schlosshauer B, Dreesmann L, Schaller HE, Sinis N. Synthetic nerve guide implants in humans: a comprehensive survey. Neurosurgery. 2006;59(4):740-748.
22. Arslantunali D, Dursun T, Yucel D, Hasirci N, Hasirci VJ. Peripheral nerve conduits: technology update. Med Devices (Auckl). 2014:405-424.
23. Verreck G, Chun I, Li Y, Kataria R, Zhang Q, Rosenblatt J, et al. Preparation and physicochemical characterization of biodegradable nerve guides containing the nerve growth agent sabeluzole. Biomaterials. 2005 ;26(11):1307-1315.
24. Janoušková O. Synthetic polymer scaffolds for soft tissue engineering. Physiol Res. 2018;67.
25. Gautam S, Ambwani S. Tissue engineering: new paradigm of biomedicine. Biosci., Biotech. Res. Asia. 2019;16(3):521-532.
26. Carvalho JL, De Carvalho PH, Gomes DA, De Goes AM. Innovative strategies for tissue engineering. Advances in Biomaterials Science and Biomedical Applications. Springer. 201;11:295.
27. Hu J, Tian L, Prabhakaran MP, Ding X, Ramakrishna S. Fabrication of nerve growth factor encapsulated aligned poly (ε-caprolactone) nanofibers and their assessment as a potential neural tissue engineering scaffold. Polymers. 2016;8(2):54.
28. Bhang SH, Jeong SI, Lee TJ, Jun I, Lee YB, Kim BS, et al. Electroactive electrospun polyaniline/poly [(L-lactide)-co-(ε-caprolactone)] fibers for control of neural cell function. Macromol Biosci. 2012;12(3):402-411.
29. Nelson DL, Balian G. The effect of retinoic acid on collagen synthesis by human dermal fibroblasts. Coll Relat Res. 1984;4(2):119-128.

30. Yen CM, Shen CC, Yang YC, Liu BS, Lee HT, Sheu ML, et al. Novel electrospun poly (ε-caprolactone)/type I collagen nanofiber conduits for repair of peripheral nerve injury. Neural Regen Res. 2019 ;14(9):1617-1625.
31. Swindle-Reilly KE, Paranjape CS, Miller CA. Electrospun poly (caprolactone)-elastin scaffolds for peripheral nerve regeneration. Prog Biomater.2014;3:1-8.
32. O'Leary C, Soriano L, Fagan-Murphy A, Ivankovic I, Cavanagh B, O'Brien FJ, et al. The fabrication and in vitro evaluation of retinoic acid-loaded electrospun composite biomaterials for tracheal tissue regeneration. Front Bioeng Biotechnol. 2020;8:190.
33. Chakrapani VY, Gnanamani A, Giridev VR, Madhusoothanan M, Sekaran G. Electrospinning of type I collagen and PCL nanofibers using acetic acid. J Appl Polym Sci. 2012 ;125(4):3221-3227.
34. Khadem Mohtaram N, Ko J, Carlson M, Byung-Guk Jun M, Willerth S. Nanofabrication of Electrospun Fibers for Controlled Release of Retinoic Acid. 8th International Conference on MicroManufacturing (ICOMM) 2013.
35. Hackett JM, Dang TT, Tsai EC, Cao X. Electrospun biocomposite polycaprolactone/collagen tubes as scaffolds for neural stem cell differentiation. Materials. 2010;3(6):3714-3728.
36. Siddiqui N, Asawa S, Birru B, Baadhe R, Rao S. PCL-based composite scaffold matrices for tissue engineering applications. Mol Biotechnol. 2018;60:506-532.
37. Mohamadi, F., Ebrahimi-Barough, S., Reza Nourani, M., Ali Derakhshan, M., Goodarzi, V., Sadegh Nazockdast, et al.Electrospun nerve guide scaffold of poly (ε caprolactone) /collagen/nanobioglass: an in vitro study in peripheral nerve tissue engineering. J Biomed Mater Res A, 2017;105(7):1960-1972.
38. Mohamadi, F., Ebrahimi-Barough, S., Nourani, M.R., Mansoori, K., Salehi, M., Alizadeh, A.A., et al. Enhanced sciatic nerve regeneration by human endometrial stem cells in an electrospun poly (ε-caprolactone)/collagen/NBG nerve conduit in rat. Artif Cells Nanomed Biotechnol. 2018;46(8):1731-1743.
39. Hackett JM, Dang TT, Tsai EC, Cao X. Electrospun biocomposite polycaprolactone/collagen tubes as scaffolds for neural stem cell differentiation. Materials. 2010;3(6):3714-3728.
40. Ahmadi P, Nazeri N, Derakhshan MA, Ghanbari H. Preparation and characterization of polyurethane/chitosan/CNT nanofibrous scaffold for cardiac tissue engineering. Int J Biol Macromol. 2021;180:590-598.
41. Nazeri N, Karimi R, Ghanbari H. The effect of surface modification of poly-lactide-co-glycolide/carbon nanotube nanofibrous scaffolds by laminin protein on nerve tissue engineering. J Biomed Mater Res A. 2021;109(2):159-169.
42. Miele D, Catenacci L, Rossi S, Sandri G, Sorrenti M, Terzi A, et al. Collagen/PCL nanofibers electrospun in green solvent by DOE assisted process. An insight into collagen contribution. Materials. 2020;13(21):4698.
43. Zander NE, Orlicki JA, Rawlett AM, Beebe TP. Surface-modified nanofibrous biomaterial bridge for the enhancement and control of neurite outgrowth. Biointerphases. 2010;5(4):149-158.
44. Huo P, Han X, Zhang W, Zhang J, Kumar P, Liu B. Electrospun nanofibers of polycaprolactone/collagen as a sustained-release drug delivery system for artemisinin. Pharmaceutics. 2021;13(8):1228.
45. Hu J, Tian L, Prabhakaran MP, Ding X, Ramakrishna S. Fabrication of nerve growth factor encapsulated aligned poly (ε-caprolactone) nanofibers and their assessment as a potential neural tissue engineering scaffold. Polymers. 2016;8(2):54.
46. Bhang SH, Jeong SI, Lee TJ, Jun I, Lee YB, Kim BS, Shin H. Electroactive electrospun polyaniline/poly [(L-lactide)-co-(ε-caprolactone)] fibers for control of neural cell function. Macromol Biosci. 2012;12(3):402-411.
47. Gümüşderelioğlu M, Dalkıranoğlu S, Aydın RS, Çakmak S. A novel dermal substitute based on biofunctionalized electrospun PCL nanofibrous matrix. J Biomed Mater Res A. 2011;98(3):461-472.
48. Chang MC, Tanaka J. FT-IR study for hydroxyapatite/collagen nanocomposite cross-linked by glutaraldehyde. Biomaterials. 2002;23(24):4811-4818.
49. Venugopal JR, Zhang Y, Ramakrishna S. In vitro culture of human dermal fibroblasts on electrospun polycaprolactone collagen nanofibrous membrane. Artif Organs.2006;30(6): 440-446.
50. Pereira AD, Pereira LG, Barbosa LA, Fialho SL, Pereira BG, Patricio PS, et al. Efficacy of methotrexate-loaded poly (ε-caprolactone) implants in Ehrlich solid tumor-bearing mice. Drug Deliv. 2013;20(3-4):168-179.
51. Afrash H, Nazeri N, Davoudi P, FaridiMajidi R, Ghanbari H. Development of a bioactive scaffold based on NGF containing PCL/chitosan nanofibers for nerve regeneration. Biointerface Res Appl Chem. 2021;11:12606-12617.
52. Chong EJ, Phan TT, Lim IJ, Zhang YZ, Bay BH, Ramakrishna S, et al. Evaluation of electrospun PCL/gelatin nanofibrous scaffold for wound healing and layered dermal reconstitution. Acta Biomater. 2007;3(3):321-330.
53. Yu W, Zhao W, Zhu C, Zhang X, Ye D, Zhang W, et al. Sciatic nerve regeneration in rats by a promising electrospun collagen/poly (ε-caprolactone) nerve conduit with tailored degradation rate. BMC Neurosci. 2011;12:1-4.
54. Jiang X, Cao HQ, Shi LY, Ng SY, Stanton LW, Chew SY. Nanofiber topography and sustained biochemical signaling enhance human mesenchymal stem cell neural commitment. Acta Biomater. 2012;8(3):1290-1302.
55. Damanik FF, van Blitterswijk C, Rotmans J, Moroni L. Enhancement of synthesis of extracellular matrix proteins on retinoic acid loaded electrospun scaffolds. J Mater Chem B. 2018 ; 6(40) : 6468-6480.